Eur. Phys. J. B (2012) 85: 279
DOI: 10.1140/epjb/e2012-30422-6

THE EUROPEAN PHYSICAL JOURNAL B

Regular Article

Superconductivity at $T_c = 44$ K in $Li_xFe_2Se_2(NH_3)_y$

E.-W. Scheidt[1], V.R. Hathwar[1], D. Schmitz[1], A. Dunbar[1], W. Scherer[1], F. Mayr[2], V. Tsurkan[2,3,a], J. Deisenhofer[2], and A. Loidl[2]

[1] CPM, Institute of Physics, University of Augsburg, 86157 Augsburg, Germany
[2] Center for Electronic Correlations and Magnetism, Institute of Physics, University of Augsburg, 86159 Augsburg, Germany
[3] Institute of Applied Physics, Academy of Sciences of Moldova, MD 2028, Chisinau, R. Moldova

Received 25 May 2012 / Received in final form 12 June 2012
Published online 8 August 2012 –

Abstract. Following a recent proposal by Burrard-Lucas et al. [arXiv:1203.5046] we intercalated FeSe with Li in liquid ammonia. We report on the synthesis of new $Li_xFe_2Se_2(NH_3)_y$ phases as well as on their magnetic and superconducting properties. We suggest that the superconducting properties of these new hybride materials appear not to be influenced by the presence of electronically-innocent $Li(NH_2)$ molecules. Indeed, high onset temperatures of 44 K and shielding fractions of almost 80% were only obtained in samples containing exclusively $Li_x(NH_3)_y$ moieties acting simultaneously as electron donors and spacer units. The c-axis lattice parameter of the new intercalated phases is strongly enhanced when compared to the alkali-metal intercalated iron selenides $A_{1-x}Fe_{2-y}Se_2$ with A = K, Rb, Cs, Tl with $T_c = 32$ K.

1 Introduction

The discovery of iron-based superconductors in 2008 [1] has increased interest to find systems that would rival the T_c records of the copper-based superconductors [2]. The highest transition temperatures of Fe based superconductors to date are in the vicinity of 56 K and were reported already within the first year after the initial discovery of the Fe based systems [3,4]. Meanwhile a variety of families have been identified [5–8] all of which share a common structural unit, namely Fe_2As_2 or Fe_2Se_2 layers which are responsible for carrying superconductivity (see [9,10] for recent reviews). The report of superconductivity in the binary chalcogenide, FeSe at about 8 K [11], has not only provided a simple model system to study the origin and the mechanism of superconductivity. It has also renewed the search for systems with a T_c above the temperature of liquid nitrogen.

First, substitution of Se by Te increased T_c to about 15 K [12–15]. Then, the critical temperature of FeSe was found to increase to 37 K under pressure [16]. A further milestone in the evolution of Fe-based superconductors was set by the synthesis of $A_{1-x}Fe_{2-y}Se_2$ single crystals with A = K, Rb, Cs, Tl and $T_c \sim 32$ K [17,18]. In addition to being superconducting these compounds exhibit iron-vacancy order in a $\sqrt{5} \times \sqrt{5} \times 1$ supercell below 580 K and local moment antiferromagnetism with large ordered moments and magnetic ordering temperatures between 470 K–560 K [18,19]. Recently, ample experimental evidence showed that these systems, which are sometimes referred to as the 245-family, are phase separated [20–24] where thin metallic Fe_2Se_2 sheets with no Fe vacancies [23] carry superconductivity at low temperatures. These metallic sheets alternate with insulating antiferromagnetic layers [24]. The fact that these natural heterostructures behave like ideal single crystals with metallic sheets almost epitaxially intergrown within the insulating antiferromagnet is best documented by the observation of the characteristic spin excitation modes of unconventional superconductors at well defined Q-values in reciprocal space by inelastic neutron scattering [25,26]. Applying pressure leads to a suppression of both antiferromagnetism and superconductivity in these systems at the same critical pressure of approximately 6 GPa [27–29]. In addition, a new superconducting phase was found to emerge at pressures beyond 12 GPa with $T_c = 48$ K [30].

Recently, reports of spurious superconductivity around 40 K appeared [31–33], and it was claimed that T_c increases with a larger distance between the FeSe layers to 44 K [33]. A completely new route for Fe chalcogenide superconductors was put forward by Ying et al. [34], who pioneered the intercalation of FeSe by alkali, alkaline-earth, and rare earth elements by an ammonothermal reaction in an autoclave with superconducting transition temperatures ranging from 30 to 46 K. Burrard-Lucas et al. [35] showed that the intercalation of FeSe with lithium in liquid ammonia leads to $T_c = 43$ K.

Following a modified intercalation approach we obtained superconducting samples with a critical onset temperature of superconductivity of 44 K and a diamagnetic shielding signal corresponding to about 80% of the sample volume. The study by Burrand-Lucas et al. stresses the

[a] e-mail: vladimir.tsurkan@physik.uni-augsburg.de

role of intercalated lithium ions, lithium amide $Li(NH_2)$ and ammonia as spacer layers. In the following we will show, however, that the presence of the lithium amide as an electronically-innocent guest species is not a prerequisite for the onset of superconductivity. The superconducting properties are controlled by electronic doping and lattice expansion due to the presence of the $Li_x(NH_3)_y$ units.

These results could be the starting point to employ tailor-made electronic donor molecules (e.g. metallocenes) which allow for a systematic variation of the donor capabilities of the guest species and the interlayer separation in Fe_2Se_2 hybrids and thus a systematic control of the critical temperatures.

2 Experimental details

Polycrystalline samples of tetragonal FeSe were synthesized from high purity Fe pieces (99.99%) and Se (99.999%) shots. Stoichiometric mixtures of the starting materials were placed in double-wall ampoules and slowly heated to 1100 °C, kept at this temperature for 48 h and then cooled with a rate of 60 °C/h to 410 °C. At 410 °C the ampoules were kept for 100 h and then quenched in ice water. X-ray diffraction and SQUID measurements documented single phase character of the materials lacking any impurity phases and displaying the appropriate tetragonal space group $P4/nmm$, with lattice constants $a = b = 0.3771$ nm and $c = 0.5524$ nm. Furthermore, a well-defined transition into the superconducting state with an onset temperature of 9.5 K was identified. The high transition temperature and the ratio of $c/a = 1.4648$ signal a composition close to $Fe_{1.02}Se$ [36]. We note, that careful inspection of powderized samples of tetragonal FeSe revealed its metastable character. Indeed, a tribochemical transition and formation of Fe_7Se_8 as a ferrimagnetic impurity [37] is observed upon grinding of tetragonal FeSe samples. Hence, excessive grinding of the samples should be avoided before the subsequent intercalation reaction in liquid ammonia.

The various intercalation reactions of tetragonal FeSe host lattices with lithium were carried out under inert gas conditions in liquid ammonia employing Schlenk techniques. In order to prevent the formation and intercalation of significant amounts of lithium amide rather small batches of FeSe (100–600 mg) were intercalated. Hence, an excess of Li metal (99.9%; Sigma Aldrich) was avoided to synthesize amide-free $Li_xFe_2Se_2(NH_3)_y$ hybride materials. Furthermore, the cooling bath temperature was always kept at about –75 °C during the intercalation period (typically 1–4 h) and the removal of the remaining NH_3 solvent was accomplished via condensation into a liquid-nitrogen cooling trap using a vacuum pump. The dry sample was allowed to warm up before the transfer to a glove box (argon inert gas) which is equipped with an inlet system adopted for the sample holders of the subsequent magnetic measurements. Hence, all sample manipulations during synthesis and physical property measurements were strictly performed under inert gas condition. Two samples with different amounts of lithium were synthesized by this approach: $Li_{0.5}Fe_2Se_2(NH_3)_{0.6}$ and $Li_{0.9}Fe_2Se_2(NH_3)_{0.5}$. Elemental analysis of the two samples yielded N:H ratios of 1:3.06 and 1:2.97, respectively, in line with the successful intercalation of $Li_x(NH_3)_y$ units and avoidance of any significant $Li(NH_2)$ impurity phases. Both samples yielded T_c-values of 44 K and shielding fractions as high as 80%. This result clearly suggests that the $Li(NH_2)$ impurities found in the materials prepared by Burrard-Lucas et al. do not trigger the superconducting properties of the $LiFe_2Se_2$ hybride phases.

Indeed, a control experiment using an excess of lithium during the intercalation process yielded a product containing significant amounts of $Li(NH_2)$ with the formal stoichiometry of $Li_{1.8}Fe_2Se_2(NH_3)[Li(NH_2)]_{0.5}$ but yielding a lower T_c of 40 K. Since the Fe_2Se_2 parent lattice only provides voids to accommodate formally one NH_3/NH_2^- moiety per formula unit it remains to be seen, whether $Li(NH_2)$ represent a true guest species or just an impurity phase. Signatures of the expected stretching and deformation modes of non-intercalated $Li(NH_2)$ were found at 3259, 1537 and 597 cm^{-1}, respectively [34], by infrared absorption measurements of $Li_{1.8}Fe_2Se_2(NH_3)[Li(NH_2)]_{0.5}$ using a standard KBr-technique and a Bruker Fourier-transform spectrometer IFS 66v/S. We therefore suggest that the electronically inert $Li(NH_2)$ moiety will not contribute to the physical properties of these hybride materials. Furthermore, the successful synthesis of samples with large shielding fractions also suggests that the intercalation process can be performed at ambient pressure and does not require ammonothermal reaction conditions in an autoclave and rather long intercalation times (2–12 days) as reported by Ying et al. [34]. This is also true for the related sodium hybrids $Na_xFe_2Se_2(NH_3)_y$ ($T_c = 45.5$ K) synthesized by the same synthetic approach as outlined for the Li intercalated samples.

Magnetization measurements were performed with a magnetic property measurement system MPMS-7 (Quantum Design), in a temperature range between 2 K to 300 K and in magnetic fields up to 7 T. All powder samples were mounted in a special Kel-F sample holder, which has a cylindrical hole with a diameter of 3 mm and a height of 3 mm. The samples were prepared in argon atmosphere and transferred to the magnetometer via an argon-lock. To determine the volume susceptibility of the intercalated samples, the density ρ was derived from the unit-cell volume based on the powder diffraction and the analytical data. The calculated density for $Li_{0.9}Fe_2Se_2(NH_3)_{0.5}$ is 3.903 g/cm^3 and for $Li_{1.8}Fe_2Se_2(NH_3)[Li(NH_2)]_{0.5}$ the value is 4.211 g/cm^3.

3 Experimental results and discussion

Phase identification and purity of the parent lattices and of the intercalated hybrid materials was controlled by powder diffraction studies using a Image Plate Guinier Camera G670 (Huber) and monochromatic $CuK_{\alpha 1}$ radiation with $\lambda = 1.540598$ Å. A flat sample holder was employed and the inherent air and moisture sensitive samples were

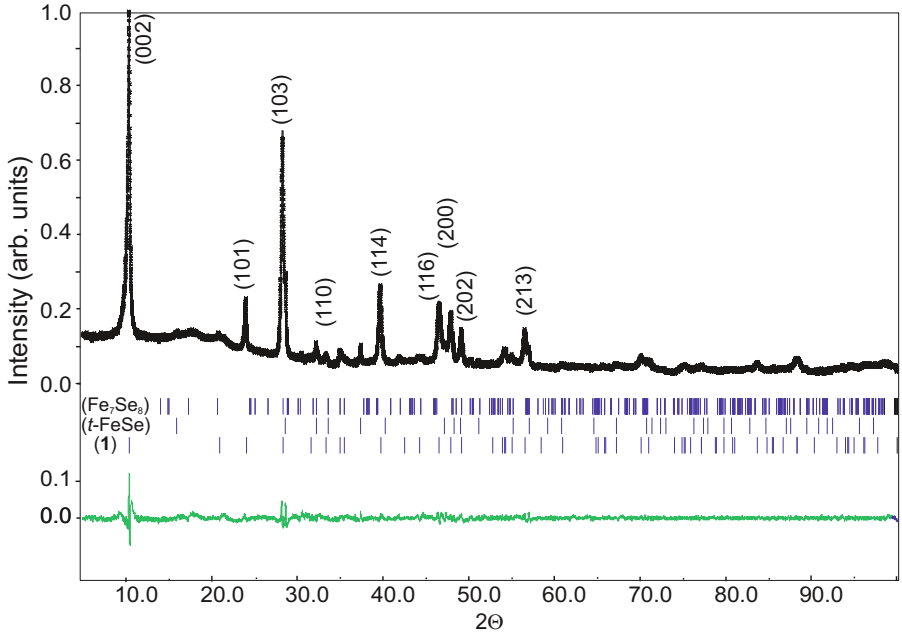

Fig. 1. (Color online) Powder diffraction pattern of $Li_{1.8}Fe_2Se_2(NH_3)[Li(NH_2)]_{0.5}$ (**1**) at room temperature. The intensity was normalized to the maximal intensity of the (002) reflection. The result of a fit using the Le-Bail method [38] is indicated as a solid line. The resulting difference pattern is indicated at the bottom of the figure. The calculated and allowed Bragg reflections of the parent compound (tetragonal FeSe), Fe_7Se_8 impurities (traces) and the intercalated hybride material (**1**) are indicated by vertical bars.

prepared inside a glove box. The samples were sealed in between two layers Mylar foil to prevent sample decomposition. Phase analysis and lattice parameter refinements were performed using the Le-Bail method for profile fitting and phase identification [38].

In Figure 1 the powder-diffraction pattern is shown for $Li_{1.8}Fe_2Se_2(NH_3)[Li(NH_2)]_{0.5}$. All Bragg intensities of the intercalated species can be indexed by a body centered tetragonal cell with $I4/mmm$ symmetry in agreement with the study by Burrard-Lucas et al. [35]. The lattice parameters seem to depend on the amount and ratio of intercalated $Li(NH_3)/Li(NH_2)$ fractions, for example, $a = b = 0.38273(6)$ nm and $c = 1.6518(3)$ nm (using space group $I4/mmm$) for $Li_{0.9}Fe_2Se_2(NH_3)_{0.5}$ and $a = b = 0.379607(8)$ nm and $c = 1.69980(11)$ nm in the case of $Li_{1.8}Fe_2Se_2(NH_3)[Li(NH_2)]_{0.5}$. Compared to the FeSe starting material the in-plane lattice constants are almost the same, being expanded by less than 1.5%. The c-axis however is enlarged by more than a factor of 3. Compared to the 245 compounds [18] the in-plane lattice constants ($a\sqrt{5}$) are slightly smaller but the c-axis is dramatically increased, a fact which strongly points toward the importance of the FeSe layer separation along c to enhance the T_c values. However, one has to keep in mind that the alkali intercalated 245 compounds exhibit critical temperatures of approximately 32 K, independent of the magnitude of the c-axis lattice change, which increases from 1.40 nm in the potassium containing compounds to 1.53 nm in the caesium intercalated compounds [18].

The temperature dependent magnetic susceptibilities of two intercalated Fe_2Se_2 samples are depicted in Figure 2 showing the respective zero-field-cooled (zfc)

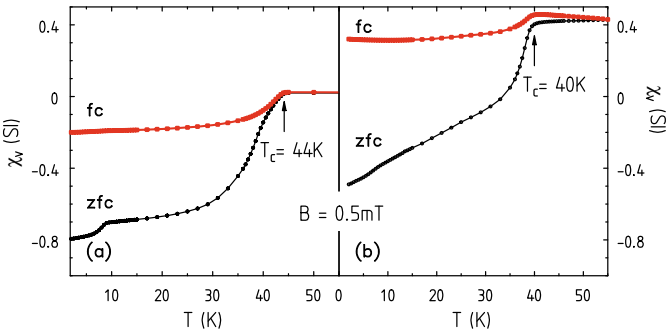

Fig. 2. (Color online) Temperature dependence of the magnetic susceptibility of intercalated FeSe samples as obtained in zero-field-cooled (zfc) and field-cooled (fc) runs. In field cooling cycles and as probing dc fields, external magnetic fields of 0.5 mT have been used. (a) Volume susceptibility of the batch with the lowest normal-state susceptibility $Li_{0.5}Fe_2Se_2(NH_3)_{0.6}$. (b) Volume susceptibility of the batch with the highest normal-state susceptibility $Li_{1.8}Fe_2Se_2(NH_3)[Li(NH_2)]_{0.5}$. The superconducting onset temperatures are indicated by arrows.

and field-cooled (fc) runs. The earth magnetic field was compensated during the zfc sequences (down to 2 K) by a procedure described in detail in [39]. In the subsequent heating run we applied a small magnetic field ($B = 0.5$ mT) to record the magnetization data up to 55 K. This procedure reflects the complete shielding effect of the sample at low temperature ($\chi_V = -1$ in the ideal case), whereas the fc measurements account for the Meissner expulsion. Figure 2 shows the temperature dependence of the volume susceptibility $\chi_V(T)$

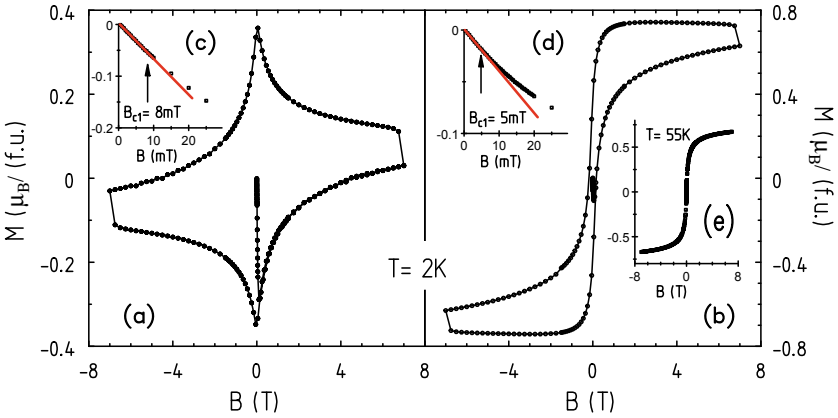

Fig. 3. (Color online) Magnetic hysteresis loop of intercalated FeSe samples at 2 K: (a) of the batch with the lowest paramagnetic background ($Li_{0.5}Fe_2Se_2(NH_3)_{0.6}$) and (b) of the batch with the highest paramagnetic background ($Li_{1.8}Fe_2Se_2(NH_3)[Li(NH_2)]_{0.5}$). The insets (c) and (d) display an expanded region of the magnetization curves which allows to estimate the lower critical field, $H_{c1}(2\ K) = 8$ mT and 5 mT in $Li_{0.5}Fe_2Se_2(NH_3)_{0.6}$ and $Li_{1.8}Fe_2Se_2(NH_3)[Li(NH_2)]_{0.5}$, respectively. Inset (e) exhibits the hysteresis loop at 55 K reflecting the ferrimagnetic contribution of the samples with the highest magnetic background.

of two selected samples, namely $Li_{0.5}Fe_2Se_2(NH_3)_{0.6}$ with the lowest normal-state susceptibility (Fig. 2a) and $Li_{1.8}Fe_2Se_2(NH_3)[Li(NH_2)]_{0.5}$ with the largest normal-state susceptibility values (Fig. 2b).

In the case of $Li_{0.5}Fe_2Se_2(NH_3)_{0.6}$ (Fig. 2a) we find a shielding fraction of about 80% as observed in the zfc measurements. Below 10 K we find the $\chi_V(T)$ signature of another superconducting transition which we ascribe to traces of the non-intercalated parent compound FeSe. The fc experiments point towards a small lower critical field and a moderate pinning effect leading to a Meissner phase which amounts approximately 20% of the sample volume. Both volume fractions seem to be significant and rather large when compared to the results by Ying et al. [34] and Burrard-Lucas et al. [35]. A well-defined onset of superconductivity in $Li_{0.5}Fe_2Se_2(NH_3)_{0.6}$ appears close to 44 K in both, the zfc and fc experiments. This is one of the highest transition temperatures reported so far in the iron-selenides at ambient pressure. For temperatures $T > T_c$ we find a small and almost vanishing paramagnetic Pauli-like magnetic susceptibility only.

In the case of $Li_{1.8}Fe_2Se_2(NH_3)[Li(NH_2)]_{0.5}$ (Fig. 2b) the relative behavior of the fc and zfc susceptibility values is similar to the amide free sample (Fig. 2a) with the exception of a lower critical temperature $T_c = 40$ K and the large normal-state susceptibility contribution of $\chi_V = 0.4$. Accordingly, the fc curve is completely shifted to positive susceptibility values. Subtracting this normal-state susceptibility of 0.4, we find that both samples exhibit shielding fractions of about 80% as observed in the zfc measurements. We will outline below that this large normal-state susceptibility might originate from a ferrimagnetic impurity (Fe_7Se_8) which is absent in $Li_{0.5}Fe_2Se_2(NH_3)_{0.6}$ but present in $Li_{1.8}Fe_2Se_2(NH_3)[Li(NH_2)]_{0.5}$ as revealed by the diffraction pattern (Fig. 1). A similar susceptibility contribution has been observed in the $Li(ND_2)$ containing sample $Li_{0.6}Fe_2Se_2(ND_2)_{0.2}(ND_3)_{0.8}$ reported by Burrad-Lucas et al. [35], which displays the highest superconducting volume fraction (40–50%) in their earlier report. In the latter case the authors found 10.3% hexagonal FeSe impurities via Rietveld analysis [35]. Consequently, the reduction or complete avoidance of FeSe impurities during sample preparation might provide one of the key control parameter of the superconducting properties of the intercalated FeSe species. Accordingly, in all compounds there seems to be a correlation between the superconducting transition temperature and the positive normal-state susceptibility values.

In order to elucidate the relationship between the superconducting state and the high positive normal-state susceptibility, magnetization measurements at 2 K and 55 K were performed. The magnetization versus magnetic field is shown in Figure 3a for $Li_{0.5}Fe_2Se_2(NH_3)_{0.6}$ and in Figure 3b for the system $Li_{1.8}Fe_2Se_2(NH_3)[Li(NH_2)]_{0.5}$ in fields up to 7 T. In case of the $LiNH_2$ free sample (Fig. 3a) the intercalated compound exhibits the typical hysteresis loop of a type-II superconductor. As in most of the 245 iron selenides and probably as a fingerprint of 2D superconductors the lower critical field is close to zero. Hence, in these systems the Meissner phase only exists close to zero external fields. The small asymmetry of the magnetization hints towards a small magnetic contribution.

This contribution is in case of the $LiNH_2$ containing sample (Fig. 3b) clearly identified as a ferrimagnetic impurity. The hysteretic loop at 55 K (Fig. 3e) shows this underlying magnetic contribution, which is most likely due to the presence of the Fe_7Se_8 impurities and/or additional free Fe-ions. The Fe_7Se_8 phase is ferrimagnetic with a saturation magnetism of 0.2 μ_B/Fe-atom and a critical temperature $T_K = 425$ K [37]. From the linear slope of this magnetization curve between –10 and 10 mT a susceptibility contribution can be derived which is in good agreement with the observed magnetic normal-state contribution in Figure 2b. In order to estimate the lower critical field B_{c1} of the samples linear fits to the initial slopes (solid lines) were performed as depicted in the insets of Figures 3c and 3d. B_{c1} at 2 K is determined by the deviation of the magnetization data from this straight line resulting in $B_{c1}(2\ K) = 0.8 \pm 0.1$ mT for $Li_{0.5}Fe_2Se_2(NH_3)_{0.6}$ and 0.5 ± 0.1 mT in the case of $Li_{1.8}Fe_2Se_2(NH_3)[Li(NH_2)]_{0.5}$.

In summary, we synthesized superconducting hybride materials $Li_xFe_2Se_2(NH_3)_y$ via intercalation of lithium in liquid ammonia. $Li_{0.5}Fe_2Se_2(NH_3)_{0.6}$ with a maximal superconducting onset temperature of 44 K is almost free of magnetic impurities with a normal-state susceptibility close to zero. The Meissner fraction of this compound

is about 20% and the shielding fraction is close to 80%. The enhancement of the critical temperature results from the significant increase of the *c*-axis lattice parameter and electron doping via lithium ions. In addition, we synthesized $Li_{1.8}Fe_2Se_2(NH_3)[Li(NH_2)]_{0.5}$. Here we found a reduced superconducting transition temperature and a significant amount of magnetic impurities. We hope that these results are the starting point to systematically vary the separation of the FeSe layers by introducing tailored electronic donor molecules.

This work has partly been supported by the DFG via the SPP 1458 (DE 1762/1-1), by TRR 80 (Augsburg-Munich) and the SPP 1178 (SCHE 487/8-3).

References

1. Y. Kamihara, T. Watanabe, M. Hirano, H. Hosono, J. Am. Chem. Soc. **130**, 3296 (2008)
2. D.N. Basov, A.V. Chubukov, Nat. Phys. **7**, 272 (2011)
3. C. Wang, L. Li, S. Chi, Z. Zhu, Z. Ren, Y. Li, Y. Wang, X. Lin, Y. Luo, S. Jiang, X. Xu, G. Cao, Z. Xu, Europhys. Lett. **83**, 67006 (2008)
4. P. Cheng, B. Shen, G. Mu, X. Zhu, F. Han, B. Zeng, H.-H. Wen, Europhys. Lett. **85**, 67003 (2009)
5. M. Rotter, M. Tegel, D. Johrendt, Phys. Rev. Lett. **101**, 107006 (2008)
6. Ch. Kant, J. Deisenhofer, A. Günther, F. Schrettle, A. Loidl, M. Rotter, D. Johrendt, Phys. Rev. B **81**, 014529 (2010)
7. X.C. Wang, Q.Q. Liu, Y.X. Lv, W.B. Gao, L.X. Yang, R.C. Yu, F.Y. Li, C.Q. Jin, Solid State Commun. **148**, 538 (2008)
8. H. Ogino, Y. Matsumura, Y. Katsura, K. Ushiyama, S. Horii, K. Kishio, J. Shimoyama, Supercond. Sci. Technol. **22**, 075008 (2009)
9. D.C. Johnston, Adv. Phys. **59**, 803 (2010)
10. G.R. Stewart, Rev. Mod. Phys. **83**, 1589 (2011)
11. F.-C. Hsu, J.-Y. Luo, K.-W. Yeh, T.-K. Chen, T.-W. Huang, P.M. Wu, Y.-C. Lee, Y.-L. Huang, Y.-Y. Chu, D.-C. Yan, M.-K. Wu, Proc. Natl. Acad. Sci. USA **105**, 14263 (2008)
12. M.H. Fang, H.M. Pham, B. Qian, T.J. Liu, E.K. Vehstedt, Y. Liu, L. Spinu, Z.Q. Mao, Phys. Rev. B **78**, 224503 (2008)
13. K.W. Yeh, T.-W. Huang, Y. Huang, T.-K. Chen, F.-C. Hsu, P.M. Wu, Y.-C. Lee, Y.-Y. Chu, C.-L. Chen, J.-Y. Luo, D.-C. Yan, M.-K. Wu, Europhys. Lett. **84**, 37002 (2008)
14. V. Tsurkan, J. Deisenhofer, A. Günther, Ch. Kant, H.-A. Krug von Nidda, F. Schrettle, A. Loidl, Eur. Phys. J. B **79**, 289 (2011)
15. A. Günther, J. Deisenhofer, Ch. Kant, H.-A. Krug von Nidda, V. Tsurkan, A. Loidl, Supercond. Sci. Technol. **24**, 045009 (2011)
16. S. Medvedev, T.M. McQueen, I.A. Troyan, T. Palasyuk, M.I. Eremets, R.J. Cava, S. Naghavi, F. Casper, V. Ksenofontov, G. Wortmann, C. Felser, Nat. Mater. **8**, 630 (2009)
17. J. Guo, S. Jin, G. Wang, S. Wang, K. Zhu, T. Zhou, M. He, X. Chen, Phys. Rev. B **82**, 180520(R) (2010)
18. F. Ye, S. Chi, Wei Bao, X.F. Wang, J.J. Ying, X.H. Chen, H.D. Wang, C.H. Dong, Minghu Fang, Phys. Rev. Lett. **107**, 137003 (2011)
19. W. Bao, Q. Huang, G.F. Chen, M.A. Green, D.M. Wang, J.B. He, X.Q. Wang, Y. Qiu, Chin. Phys. Lett. **28**, 086104 (2011)
20. A. Ricci, N. Poccia, G. Campi, B. Joseph, G. Arrighetti, L. Barba, M. Reynolds, M. Burghammer, H. Takeya, Y. Mizuguchi, Y. Takano, M. Colapietro, N.L. Saini, A. Bianconi, Phys. Rev. B **84**, 060511 (2011)
21. W. Li, H. Ding, P. Deng, K. Chang, C. Song, K. He, L. Wang, X. Ma, J.-P. Hu, X. Chen, Q.-K. Xue, Nat. Phys. **8**, 126 (2012)
22. V. Ksenofontov, G. Wortmann, S.A. Medvedev, V. Tsurkan, J. Deisenhofer, A. Loidl, C. Felser, Phys. Rev. B **84**, 180508 (2011)
23. Y. Texier, J. Deisenhofer, V. Tsurkan, A. Loidl, D.S. Inosov, G. Friemel, J. Bobroff, Phys. Rev. Lett. **108**, 237002 (2012)
24. A. Charnukha, A. Cvitkovic, T. Prokscha, D. Pröpper, N. Ocelic, A. Suter, Z. Salman, E. Morenzoni, J. Deisenhofer, V. Tsurkan, A. Loidl, B. Keimer, A.V. Boris, Phys. Rev. Lett. **109**, 017003 (2012)
25. J.T. Park, G. Friemel, Y. Li, J.-H. Kim, V. Tsurkan, J. Deisenhofer, H.-A. Krug von Nidda, A. Loidl, A. Ivanov, B. Keimer, D.S. Inosov, Phys. Rev. Lett. **107**, 177005 (2011)
26. G. Friemel, J.T. Park, T.A. Maier, V. Tsurkan, Y. Li, J. Deisenhofer, H.-A. Krug von Nidda, A. Loidl, A. Ivanov, B. Keimer, D.S. Inosov, Phys. Rev. B **85**, 140511(R) (2012)
27. M. Gooch, B. Lv, L.Z. Deng, T. Muramatsu, J. Meen, Y.Y. Xue, B. Lorenz, C.W. Chu, Phys. Rev. B **84**, 184517 (2011)
28. J. Guo, X. Chen, C. Zhang, J. Guo, X. Chen, Q. Wu, D. Gu, P. Gao, X. Dai, L. Yang, H. Mao, L. Sun, Z. Zhao, Phys. Rev. Lett. **108**, 197001 (2012)
29. V. Ksenofontov, S. Medvedev, L.M. Schoop, G. Wortmann, T. Palasyuk, V. Tsurkan, J. Deisenhofer, A. Loidl, C. Felser, Phys. Rev. B **85**, 214519 (2012)
30. L. Sun, X. Chen, J. Guo, P. Gao, H. Wang, M. Fang, X. Chen, G. Chen, Q. Wu, C. Zhang, D. Gu, X. Dong, K. Yang, A. Li, X. Dai, H. Mao, Z. Zhao, Nature **483**, 67 (2012)
31. M. Fang, H. Wang, C. Dong, Z. Li, C. Feng, J. Chen, H.Q. Yuan, Europhys. Lett. **94**, 27009 (2011)
32. D.M. Wang, J.B. He, T.-L. Xia, G.F. Chen, Phys. Rev. B **83**, 132502 (2011)
33. A.M. Zhang, T.L. Xia, W. Tong, Z.R. Yang, Q.M. Zhang, `arXiv:1203.1533`
34. T.P. Ying, X.L. Chen, G. Wang, S.F. Jin, T.T. Zhou, X.F. Lai, H. Zhang, W.Y. Wang, Sci. Rep. **2**, 426 (2012)
35. M. Burrard-Lucas, D.G. Free, S.J. Sedlmaier, J.D. Wright, S.J. Cassidy, Y. Hara, A.J. Corkett, T. Lancaster, P.J. Baker, S.J. Blundell, S.J. Clarke, `arXiv:1203.5046`
36. T.M. McQueen, Q. Huang, V. Ksenofontov, C. Felser, Q. Xu, H. Zandbergen, Y.S. Hor, J. Allred, A.J. Williams, D. Qu, J. Checkelsky, N.P. Ong, R.J. Cava, Phys. Rev. B **79**, 014522 (2009)
37. K. Adachi, J. Phys. Soc. Jpn **16**, 2187 (1961)
38. A. LeBail, Powder Diffraction **14**, 249 (2004)
39. M. Presnitz, M. Herzinger, E.-W. Scheidt, W. Scherer, M. Baenitz, M. Marz, Measur. Sci. Technol. **23**, 085002 (2012)